AIAA JOURNAL
Vol. 44, No. 8, August 2006

Analysis Tools for Adhesively Bonded Composite Joints, Part 2: Unified Analytical Theory

Jian Zhang*
Collier Research Corporation, Hampton, Virginia 23669
Brett A. Bednarcyk†
Ohio Aerospace Institute, Brookpark, Ohio 44142
Craig Collier‡ and Phil Yarrington§
Collier Research Corporation, Hampton, Virginia 23669
and
Yogesh Bansal‖ and Marek-Jerzy Pindera¶
University of Virginia, Charlottesville, Virginia 22903

DOI: 10.2514/1.15664

Adhesively bonded joints are currently of interest to the aerospace field due to the heavy reliance on bonded composite structures in new aircraft designs. In response, tools for joint analysis have been developed and examined in this two-part paper. In Part 1, a higher-order theory, considering an explicit discretization of the joint geometry, was investigated. In Part 2, a method for multiaxial stress analysis of composite joints is developed based on Mortensen's unified approach, with considerable extension to accommodate transverse in-plane strain and hygrothermal loads and most importantly, to compute the in-plane and interlaminar stresses in the adherends. Compared with other analytical methods for bonded joint analysis, the present method is capable of handling more general situations, including various joint geometries, linear and nonlinear adhesives, asymmetric and unbalanced laminates, and various loading and boundary conditions. The method has been implemented within the commercially available HyperSizer® structural analysis software. Through comparison to finite element and analytical results, it is shown that the new HyperSizer joint analysis method is efficient and accurate and can serve as a capable tool for joint analysis in preliminary design, where rapid and generally accurate stress field estimates, as well as joint strengths and margins are needed.

I. Introduction

Adhesive composite joints have been widely used in modern lightweight flight and space vehicle structures and will be used more heavily in the next generation of aircraft, such as the joint strike fighter, the long range strike aircraft, and new unmanned aerial vehicles. However, joining composite structures using adhesive bonding remains a challenging problem because performance of bonded joints is severely influenced by the characteristics of composite laminate adherends, which usually have low interlaminar strengths. The interlaminar stresses induced in the vicinity of the bondline leading edges of joints can then cause delamination of the laminated adherends. Thus, accurate multiaxial stress analysis is essential for understanding failure of bonded composite joints. While tools exist for rapid design, analysis, and sizing of aerospace structures from the level of the vehicle to the level of the stiffened panel component (HyperSizer®, Collier Research Corp., 1998) [1], a weak link in the design process remains the automated sizing of joints between structural components. Hence, methods that address this gap are needed to enable rapid estimates of joint stress fields, strengths, and margins of safety.

The adhesively bonded joint problem is typically approached in one of two ways: with finite element analysis or through analytical modeling. Finite element analysis has the advantage of geometric flexibility and the availability of commercial finite element codes. Examples of finite element investigations of adhesively bonded composite joints include Kairouz and Matthews [2], Shenoi and Hawkins [3], Tsai et al. [4], Yamazaki and Tsubosaka [5], Tong [6], Li et al. [7], Apalak et al. [8], Krueger et al. [9,10], and Bogdanovich and Kizhakkethara [11], among others. The literature shows that standard *h*-based finite element codes do a good job of predicting the local stress fields within adhesively bonded joints under arbitrary loading conditions. However, this approach can suffer in terms of efficiency, and its high level of mesh dependence limits its applicability to design and sizing, where a large number of different joint configurations may need to be considered and analyzed. *P*-based finite element codes such as StressCheck** improve local field predictions by altering the order of the elements' polynomials rather than requiring successively finer element meshes to capture concentrations. In light of this, the Composites Affordability Initiative has selected StressCheck as a potential design tool for adhesively bonded joints.

The analytical approach to adhesively bonded joint analysis typically employs simplifying assumptions in terms of the joint geometry, loading, and resultant local fields in order to formulate an efficient closed-form elasticity solution for the local fields in the joint region. The analytical approach has its roots in classical shear-lag analysis of Volkersen [12] and the work of Goland and Reissner [13], who accounted for bending in the analysis of a bonded single lap joint. Hart-Smith [14–19] extended these solutions to account for the inelastic behavior of the adhesive and considered many joint and adherend configurations. However, the Hart-Smith formulations are limited in the applied loading considered and the 1-D treatment of the adherends with an effective stiffness in the joint direction. Delale

Received 21 January 2005; revision received 16 November 2005; accepted for publication 22 November 2005. Copyright © 2006 by Collier Research Corp.. Published by the American Institute of Aeronautics and Astronautics, Inc., with permission. Copies of this paper may be made for personal or internal use, on condition that the copier pay the $10.00 per-copy fee to the Copyright Clearance Center, Inc., 222 Rosewood Drive, Danvers, MA 01923; include the code $10.00 in correspondence with the CCC.

*Research Engineer, 2 Eaton Street, Suite 504. Member AIAA.
†Senior Scientist, 22800 Cedar Point Road. Member AIAA.
‡Senior Research Engineer, 2 Eaton Street, Suite 504. Senior Member AIAA.
§Senior Research Engineer, 2 Eaton Street, Suite 504. Member AIAA.
‖Research Assistant, Applied Mechanics, Thornton Hall B228, 351 McCormick Road.
¶Professor, Department of Civil Engineering.

**ESRD, Inc., http://www.esrd.com, St. Louis, MO [cited 14 May 2003].

et al. [20] developed a closed-form solution for lap-shear joints with orthotropic adherends by using classical plate theory. Oplinger [21] developed a layered beam analysis, which included treatment of large deflection of joint overlap. However, the above analytical methods developed for bonded joints analysis mainly focused on obtaining adhesive stresses, while generally ignoring stresses in the adherends, particularly the interlaminar stresses, which are known to be key contributors to failure of laminated adherends.

More recently, Mortensen [22] and Mortensen and Thomsen [23,24] presented a unified analytical approach to analyze an array of common bonded joint configurations for more general loading conditions. Mortensen's treatment also considers arbitrary laminate adherends (based on their ABD matrices) and solves for the distributions of normal and shear force and moment resultants along the joint in all adherends (as well as peel and shear stress distributions in the adhesive). Further, through the application of an efficient solution algorithm, convergence issues that arise in Hart-Smith's formulation have been overcome. However, the full stress field throughout the adherends was still not determined through Mortensen's approach [22].

The main objective of this paper is to present a new capability for the design and analysis of bonded joints based on extensions of Mortensen's unified approach. This new tool has been incorporated into the HyperSizer® structural sizing software framework. The basic features of Mortensen's approach have been retained. A wide range of joint types may be considered, and the adherends, which were originally modeled as classical laminates in cylindrical bending, can be unbalanced and asymmetric laminates. Both linear and nonlinear behavior of the adhesive layer is admitted in the analysis. For linear analysis, the adhesive layer is modeled as continuously distributed linear tension/compression and shear springs (i.e., a traction-separation law). Inclusion of nonlinear adhesive behavior in the analysis is accomplished through the use of a secant modulus approach for the nonlinear tensile stress–strain relationship in conjunction with a yield criterion. Finally, the equilibrium equations for each joint are derived, and by combination of these equations and relations, the set of governing ordinary differential equations is obtained. The governing system of equations is solved numerically using a multisegment method of integration [22], yielding laminate-level fields and adhesive stresses that vary along the joint in each adherend.

The considerable extensions that have been made to the original Mortensen's approach have rendered the method more suitable for design of adhesive joints in real aerospace structures. The formulation has been extended from strict cylindrical bending to generalized cylindrical bending, allowing an arbitrary constant strain to be applied in the out-of-plane direction. In addition, hygrothermal effects have been incorporated into the method. Most importantly, the method now computes local full multiaxial stress fields in each ply of each adherend, which vary along the joint. This is accomplished by directly calculating in-plane stress components in the adherend plies from the laminate constitutive equations derived from the classical lamination theory (CLT). Then, interlaminar stress fields within the adherends are obtained through integration of the pointwise equilibrium equations. Given the realistic multiaxial local stress fields at the ply level within each adherend, failure criteria can be employed to predict bond strength, and thus design the joint to increase its strength.

The present investigation employs HyperSizer's new joint analysis capabilities to analyze composite bonded doubler joints. Results for in-plane and out-of-plane stresses within the adherends, together with adhesive stresses, are plotted and compared with *p*-based finite element results, both of which considered elastic adhesive behavior. The results indicate that HyperSizer is an efficient and generally accurate tool for the structural analysis of adhesively bonded joints.

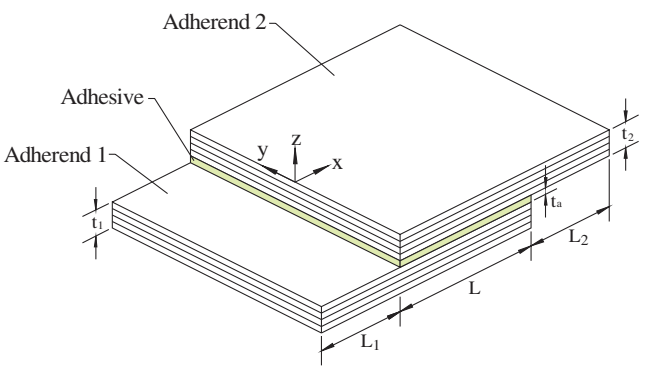

Fig. 1 Schematic illustration of an adhesive single lap joint with straight adherends in the overlap zone.

II. Description of the Joint Analysis Method

A. Basic Assumptions for the Structural Modeling of Bonded Joints

The HyperSizer joint analysis method for bonded joint analysis is developed based upon Mortensen's unified approach, but with considerable extension to compute in-plane and interlaminar stresses in the adherends and to accommodate a constant applied transverse strain and hygrothermal loads. The basic assumptions of the method for the structural modeling of bonded joints are summarized in the following:

The adherends: 1) Plates in generalized cylindrical bending, which allows for uniform strain applied in the transverse direction; 2) Generally orthotropic laminates governed by the classical lamination theory; 3) The strains are small, and the rotations are very small.

The adhesive layer: 1) Modeled as continuously distributed linear tension/compression and shear springs via traction-separation relations; 2) Inclusion of nonlinear adhesive behavior via a nonlinear secant modulus approach.

Loading and boundary conditions: 1) General boundary and loading conditions. One of each pair in the following can be applied at the joint boundaries: a) longitudinal displacement (midplane) or axial force (u_0 or N_{xx}); b) in-plane transverse displacement or shear force (v_0 or N_{xy}); c) vertical deflection or transverse shear force (w or Q_x); d) longitudinal curvature or moment (β_x or M_{xx}); 2) hygrothermal load: uniform temperature change ΔT, uniform moisture content change Δc; 3) in the in-plane transverse (y) direction, uniform strain e_0 can be applied; 4) reaction forces (and moments) in y direction: M_{yy}, M_{xy}, N_{yy} are calculated.

The method can be generally applied to eight types of bonded joints: single-lap, double-lap joints with straight or scarfed adherends, bonded doubler with straight or stepped adherends, single- double-sided scarfed lap joints.

B. Adherends as Plates in Generalized Cylindrical Bending

Modified from Mortensen's [22] original cylindrical bending assumptions for the adherends, the generalized cylindrical bending conditions treat the adherends and joint as a wide plate, where the longitudinal (x direction) displacement and vertical deflection are functions of the longitudinal (x) coordinate only, while the in-plane transverse (y direction) displacement can accommodate generalized plane strains in addition to the longitudinal field (see Fig. 1). As a consequence, the longitudinal displacements and deflection will be uniform along the width (y) direction, while the in-plane transverse displacement varies linearly along the width (y) direction. Thus, the displacement field is given by

$$u_0^i = u_0^i(x), \qquad v_0^i = e_0^i y + v_0^i(x), \qquad w^i = w^i(x) \tag{1}$$

where u_0 is the midplane displacement in the longitudinal direction (x direction), v_0 is the midplane displacement in the width direction (y direction), w is the displacement in the out-of-plane transverse direction (z direction), and e_0 is the uniform strain in the y direction. The displacement components in each laminate, u_0, v_0, w, are all defined relative to the middle surface of each laminate, and i corresponds to the laminate/adherend number.

Considering that the adherends are subjected to both mechanical and nonmechanical loads (i.e., hygrothermal strains), the constitutive equations for the laminated adherends are given by

$$
\begin{aligned}
N^i_{xx} &= A^i_{11}u^i_{0,x} + A^i_{12}e^i_0 + A^i_{16}v^i_{0,x} - B^i_{11}w^i_{,xx} - N^{i*}_{xx},\\
N^i_{yy} &= A^i_{12}u^i_{0,x} + A^i_{22}e^i_0 + A^i_{26}v^i_{0,x} - B^i_{12}w^i_{,xx} - N^{i*}_{yy},\\
N^i_{xy} &= A^i_{16}u^i_{0,x} + A^i_{26}e^i_0 + A^i_{66}v^i_{0,x} - B^i_{16}w^i_{,xx} - N^{i*}_{xy},\\
M^i_{xx} &= B^i_{11}u^i_{0,x} + B^i_{12}e^i_0 + B^i_{16}v^i_{0,x} - D^i_{11}w^i_{,xx} - M^{i*}_{xx},\\
M^i_{yy} &= B^i_{12}u^i_{0,x} + B^i_{22}e^i_0 + B^i_{26}v^i_{0,x} - D^i_{12}w^i_{,xx} - M^{i*}_{yy},\\
M^i_{xy} &= B^i_{16}u^i_{0,x} + B^i_{26}e^i_0 + B^i_{66}v^i_{0,x} - D^i_{16}w^i_{,xx} - M^{i*}_{xy}
\end{aligned}
\tag{2}
$$

where i represents the adherend number and A^i_{jk}, B^i_{jk}, and D^i_{jk} ($j, k = 1, 2, 6$) are the extensional, coupling, and flexural rigidities. N^i_{xx}, N^i_{yy}, and N^i_{xy} are the in-plane force resultants and M^i_{xx}, M^i_{yy} and M^i_{xy} are the moment resultants. N^{i*}_{xx}, N^{i*}_{yy} and N^{i*}_{xy} are the in-plane hygrothermal force resultants, whereas M^{i*}_{xx}, M^{i*}_{yy}, and M^{i*}_{xy} are the hygrothermal moment resultants. The expression of the hygrothermal terms are given by

$$
\begin{aligned}
N^*_n &= \sum_{k=1}^{N}\left\{\bar{Q}^{(k)}_{nm}\cdot\varepsilon^{(k)*}_m\cdot t_k\right\} \quad \text{and}\\
M^*_n &= \sum_{k=1}^{N}\left\{\bar{Q}^{(k)}_{nm}\cdot\varepsilon^{(k)*}_m\cdot(z^2_k - z^2_{k-1})/2\right\}
\end{aligned}
\tag{3}
$$

where $\varepsilon^{(k)*}_m$ is the in-plane hygrothermal strain vector in each ply, i.e., $\varepsilon^{(k)*}_m = \alpha^{(k)}_m\Delta T + \beta^{(k)}_m\Delta c$. Note that the subscripts ", x" and ", xx" in Eq. (2) indicate first and second derivatives with respect to x, respectively, $\alpha^{(k)}_m$ and $\beta^{(k)}_m$ are the coefficients of thermal and moisture expansion, and ΔT and Δc are the changes in temperature and moisture content.

For the advanced joint types such as a scarfed or stepped lap the rigidities A^i_{jk}, B^i_{jk}, and D^i_{jk} ($j, k = 1, 2, 6$) are determined as functions of the longitudinal (x) direction of the joint within the overlap zone, since the adherend thicknesses vary within the overlap. From the Kirchhoff-Love assumptions, the following kinematic relations for the laminates are derived:

$$
u^i = u^i_0 + z\beta^i_x, \qquad \beta^i_x = -w^i_{,x}, \qquad \beta^i_y = 0 \tag{4}
$$

where u^i is the longitudinal displacement, u^i_0 is the longitudinal displacement of the midplane, and w_i is the vertical displacement of the ith adherend. β^i_x and β^i_y are the slopes in the two directions.

C. Constitutive Relations for the Adhesive Layer

1. *Linear Spring Adhesive Model*

The coupling between the adherends is established through the constitutive relations for the adhesive layer, which, as a first approximation, is assumed to be homogeneous, isotropic, and linearly elastic. The constitutive relations for the adhesive layer are established by use of a two-parameter traction-separation approach, where the adhesive layer is assumed to be composed of continuously distributed shear and tension/compression springs. The constitutive relations of the adhesive layer are given by

$$
\begin{aligned}
\tau_{ax} &= G_a\cdot\gamma_{ax} = (G_a/t_a)(u^i - u^j),\\
\tau_{ay} &= G_a\cdot\gamma_{ay} = (G_a/t_a)(v^i - v^j),\\
\sigma_a &= E_a\cdot\epsilon_{az} = (E_a/t_a)(w^i - w^j)
\end{aligned}
\tag{5}
$$

where i and j are the adherend numbers, τ_{ax}, τ_{ay}, σ_a, γ_{ax}, γ_{ay}, and ε_{az} are the adhesive shear and normal stresses and strains, and G_a and E_a are the shear and elastic modulus of the adhesive layer.

2. *Nonlinear Adhesive Model*

Most polymeric structural adhesives exhibit inelastic behavior in the sense that local permanent plastic strains are induced even at low levels of external loading. Thus, the assumption of linear elasticity of the adhesive is an approximation and nonlinear adhesive behavior must be considered if a more realistic response of bonded joints is sought. The nonlinear adhesive behavior can be modeled with a measured true stress-strain curve, either in pure tension or in pure shear, and a mathematical model that takes the multiaxial stress state into account. The measured stress-strain curves can be characterized by a variety of mathematical models for the sake of analytical and numerical analysis. In HyperSizer, some most commonly used mathematical models are employed to characterize the nonlinear behavior of adhesives, for example, elastic-perfectly plastic, bilinear, and Ramburg–Osgood. The analysis of nonlinear adhesives and the related solution procedures is described fully in an AFRL report [25].

D. Equilibrium Equations

The equilibrium equations are derived based on equilibrium elements inside and outside the overlap zone for each of the considered joint types. The equilibrium equations are derived for plates in generalized cylindrical bending. The general equilibrium equations outside the overlap zone for each of the adherends (Fig. 1) are

$$
\begin{aligned}
&N^i_{xx,x} = 0\\
&N^i_{xy,x} = 0\\
&Q^i_{x,x} = 0 \quad \text{outside the overlap zone}\\
&M^i_{xx,x} = Q^i_x\\
&M^i_{xy,x} = Q^i_y
\end{aligned}
\tag{6}
$$

where i corresponds to the adherends, in general, $i = 1, 2, 3$.

In generalized cylindrical bending the force and moment resultants are only functions of the longitudinal coordinate x, and their derivatives with respect to the width direction y are all equal to zero. The equilibrium equations derived inside the overlap zones can be divided into the following two groups: 1) joints with one adhesive layer inside the overlap zone, 2) joints with two adhesive layers inside the overlap zone. These two groups are further divided into joints with straight or scarfed adherends within the overlap. However, in the following only the equilibrium equations for joints with two straight adherends within the over lap will be shown, i.e., single-lap joint (see Fig. 1), bonded doubler and single sided stepped-lap joint. For a full description of the derivation of the equilibrium equations for the rest of the joint types, see Mortensen [22].

$$
\begin{aligned}
N^1_{xx,x} &= -\tau_{ax}, \qquad N^2_{xx,x} = \tau_{ax},\\
N^1_{xy,x} &= -\tau_{ay}, \qquad N^2_{xy,x} = \tau_{ay},\\
Q^1_{x,x} &= -\sigma_a, \qquad Q^2_{x,x} = \sigma_a,\\
M^1_{xx,x} &= Q^1_x - \tau_{ax}\cdot\frac{t_1(x) + t_a}{2}, \qquad M^2_{xx,x} = Q^2_x - \tau_{ax}\cdot\frac{t_2(x) + t_a}{2},\\
M^1_{xy,x} &= Q^1_y - \tau_{ay}\cdot\frac{t_1(x) + t_a}{2}, \qquad M^2_{xy,x} = Q^2_y - \tau_{ay}\cdot\frac{t_2(x) + t_a}{2}
\end{aligned}
\tag{7}
$$

where $t_1(x)$ and $t_2(x)$ are the adherend thicknesses and t_a is the adhesive layer thickness. For single-lap joints and bonded doubler joints the adherend thicknesses remain the same in the entire overlap zone; for single sided stepped-lap joints, the adherend thicknesses may change inside the overlap zone between each step.

From the equations given above, it is possible to form a complete system of governing equations for each of the bonded joint configurations. That is, combination of the constitutive and kinematic relations, together with the constitutive relations for the adhesive layers, and the equilibrium equations lead to a set of eight coupled linear first-order ordinary differential equations describing the system behavior of each of the adherends. The system equations can be solved numerically by using Mortensen's multisegment method. For details on the system of governing equations and the multisegment method, see Mortensen [22].

E. In-Plane Stresses in the Adherends

The laminate layup and associated coordinate system is shown in Fig. 2. The in-plane stresses and strains in the laminated adherends can be obtained directly from CLT, in which the Kirchhoff–Love linear assumption is applied, i.e., $\gamma_{yz} = \gamma_{zx} = 0$ and $\varepsilon_z = 0$. This assumption leads to the linear relation between the displacement field of the laminate and the midplane displacement,

$$w(x,y,z) = w^0, \qquad u(x,y,z) = u^0 - z\frac{\partial w}{\partial x}, \qquad v(x,y,z) = v^0 - z\frac{\partial w}{\partial y} \tag{8}$$

The in-plane strain fields in each laminate can thus be derived from the standard kinematic relations. They are

$$\begin{aligned} \varepsilon_x &= \frac{\partial u}{\partial x} = \frac{\partial u^0}{\partial x} + z\left(-\frac{\partial^2 w}{\partial x^2}\right) = \varepsilon_x^0 + z\kappa_x, \\ \varepsilon_y &= \frac{\partial v}{\partial y} = \frac{\partial v^0}{\partial y} + z\left(-\frac{\partial^2 w}{\partial y^2}\right) = \varepsilon_y^0 + z\kappa_y, \\ \gamma_{xy} &= \frac{\partial v}{\partial x} + \frac{\partial u}{\partial y} = \frac{\partial v^0}{\partial x} + \frac{\partial u^0}{\partial y} + z\left(-2\frac{\partial^2 w}{\partial x \partial y}\right) = \gamma_{xy}^0 + z\kappa_{xy} \end{aligned} \tag{9}$$

where $\varepsilon^0 = \{\varepsilon_x^0, \varepsilon_y^0, \varepsilon_z^0\}$ is the strain of the midplane and $\kappa = \{\kappa_x, \kappa_y, \kappa_{xy}\}$ is the curvature of the midplane. The in-plane strain of an arbitrary point in the laminate can be obtained through Eq. (9) once the midplane strain is known. The latter can be determined from the overall equilibrium and constitutive equation of the laminate.

Under the assumption of generalized cylindrical bending, the midplane displacements are given in the following forms:

$$u^0 = u^0(x), \qquad v^0 = e_0 y + v^0(x), \qquad w^0 = w^0(x) \tag{10}$$

Thus, Eq. (9) can be reduced to

$$\begin{aligned} \varepsilon_{xx} &= \frac{\partial u^0}{\partial x} + z\left(-\frac{\partial^2 w}{\partial x^2}\right) = u^0_{,x} + z\beta_{x,x}, \\ \varepsilon_{yy} &= \frac{\partial v^0}{\partial y} + z\left(-\frac{\partial^2 w}{\partial y^2}\right) = e_0, \\ \gamma_{xy} &= \frac{\partial v^0}{\partial x} + \frac{\partial u^0}{\partial y} + z\left(-2\frac{\partial^2 w}{\partial x \partial y}\right) = v^0_{,x} \end{aligned} \tag{11}$$

The in-plane stress components of the laminated adherends can be obtained through the constitutive equation for each ply. Including the hygrothermal effect, the in-plane stresses of the kth ply are given by

$$\begin{bmatrix} \sigma_{xx} \\ \sigma_{yy} \\ \tau_{xy} \end{bmatrix}^{(k)} = \begin{bmatrix} \bar{Q}_{11} & \bar{Q}_{12} & \bar{Q}_{16} \\ \bar{Q}_{21} & \bar{Q}_{22} & \bar{Q}_{26} \\ \bar{Q}_{61} & \bar{Q}_{62} & \bar{Q}_{66} \end{bmatrix}^{(k)} \left\{ \begin{bmatrix} \varepsilon_{xx} \\ \varepsilon_{yy} \\ \gamma_{xy} \end{bmatrix} - \begin{bmatrix} \varepsilon_{xx}^* \\ \varepsilon_{yy}^* \\ \gamma_{xy}^* \end{bmatrix} \right\}^{(k)} \tag{12}$$

where ε_{ij}^* is the hygrothermal strain, which is given by

$$\begin{bmatrix} \varepsilon_{xx}^* \\ \varepsilon_{yy}^* \\ \gamma_{xy}^* \end{bmatrix} = \Delta T \begin{bmatrix} \alpha_x \\ \alpha_y \\ \alpha_s \end{bmatrix} + \Delta c \begin{bmatrix} \zeta_x \\ \zeta_y \\ \zeta_s \end{bmatrix} \tag{13}$$

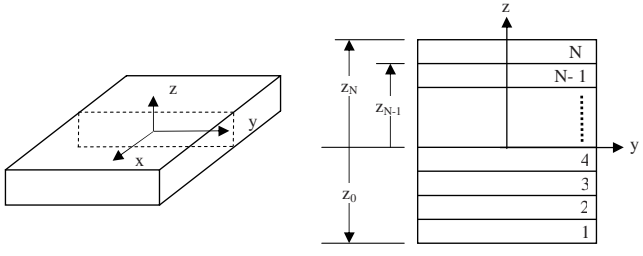

Fig. 2 Layup of a laminate and the coordinate system.

where α_j and ζ_j are the coefficients of thermal and moisture expansion, respectively.

F. Out-of-Plane (Interlaminar) Stresses in the Adherends

Even though CLT does not account for the out-of-plane response, the out-of-plane stresses can be calculated approximately using the local equilibrium equations. Without body force, the standard equilibrium equations are written as

$$\frac{\partial \sigma_{xx}}{\partial x} + \frac{\partial \tau_{xy}}{\partial y} + \frac{\partial \tau_{xz}}{\partial z} = 0, \qquad \frac{\partial \tau_{xy}}{\partial x} + \frac{\partial \sigma_{yy}}{\partial y} + \frac{\partial \tau_{yz}}{\partial z} = 0, \qquad \frac{\partial \sigma_{zz}}{\partial z} + \frac{\partial \tau_{yz}}{\partial y} + \frac{\partial \tau_{xz}}{\partial x} = 0 \tag{14}$$

Under the assumptions of generalized cylindrical bending, $\partial\sigma_{yy}/\partial y = \partial\tau_{yz}/\partial y = \partial\tau_{xy}/\partial y = 0$. Thus, the out-of-plane stress components can be obtained via integration of the simplified equilibrium equations Eq. (14),

$$\tau_{xz} = -\int_{\text{free surface}}^{z} \left(\frac{\partial \sigma_{xx}}{\partial x}\right) \mathrm{d}z, \qquad \tau_{yz} = -\int_{\text{free surface}}^{z} \left(\frac{\partial \tau_{xy}}{\partial x}\right) \mathrm{d}z, \qquad \sigma_{zz} = -\int_{\text{free surface}}^{z} \left(\frac{\partial \tau_{xz}}{\partial x}\right) \mathrm{d}z \tag{15}$$

by requiring these stress components to vanish at the adherend free surfaces. One simple way to calculate the out-of-plane stresses is to integrate Eq. (15) numerically. However, in the present joint formulation, large oscillations result due to lack of continuity of the x derivatives of the solutions of $\{u^0, v^0, w^0, \beta_x, N_{xx}, N_{xy}, M_{xx}, Q_x\}$ computed by using Mortensen's multisegment integration method [22]. To overcome this oscillation problem, some algebra is required to avoid using discontinuous numerical derivatives from the multisegment solutions. First, Eq. (12) is expanded and the in-plane stress components σ_{xx} and τ_{xy} are written as

$$\begin{aligned} \sigma_{xx}^{(k)} &= \bar{Q}_{11}^{(k)}\left[\varepsilon_{xx}^{(k)} - \varepsilon_{xx}^{(k)*}\right] + \bar{Q}_{12}^{(k)}\left[\varepsilon_{yy}^{(k)} - \varepsilon_{yy}^{(k)*}\right] \\ &\quad + \bar{Q}_{16}^{(k)}\left[\gamma_{xy}^{(k)} - \gamma_{xy}^{(k)*}\right] \\ &= \bar{Q}_{11}^{(k)}\left\{\left(u^0_{,x} + z^{(k)}\beta_{x,x}\right) - \varepsilon_{xx}^{(k)*}\right\} + \bar{Q}_{12}^{(k)}\left[e_0 - \varepsilon_{yy}^{(k)*}\right] \\ &\quad + \bar{Q}_{16}^{(k)}\left[v^0_{,x} - \gamma_{xy}^{(k)*}\right] \end{aligned} \tag{16}$$

$$\begin{aligned} \tau_{xy}^{(k)} &= \bar{Q}_{16}^{(k)}\left[\varepsilon_{xx}^{(k)} - \varepsilon_{xx}^{(k)*}\right] + \bar{Q}_{26}^{(k)}\left[\varepsilon_{yy}^{(k)} - \varepsilon_{yy}^{(k)*}\right] + \bar{Q}_{66}^{(k)}\left[\gamma_{xy}^{(k)} - \gamma_{xy}^{(k)*}\right] \\ &= \bar{Q}_{16}^{(k)}\left\{\left(u^0_{,x} + z^{(k)}\beta_{x,x}\right) - \varepsilon_{xx}^{(k)*}\right\} + \bar{Q}_{26}^{(k)}\left[e_0 - \varepsilon_{yy}^{(k)*}\right] \\ &\quad + \bar{Q}_{66}^{(k)}\left[v^0_{,x} - \gamma_{xy}^{(k)*}\right] \end{aligned} \tag{17}$$

Assuming the hygrothermal strains are constant in each ply, the derivatives of σ_{xx} and τ_{xy} and the integrals appearing in Eq. (15) are then given by

$$\frac{\partial \sigma_{xx}^{(k)}}{\partial x} = \bar{Q}_{11}^{(k)}[u^0_{,xx} + z^{(k)}\beta_{x,xx}] + \bar{Q}_{16}^{(k)}[v^0_{,xx}] \tag{18a}$$

$$\int_{\text{free}}^{z} \frac{\partial \sigma_{xx}^{(k)}}{\partial x}\,\mathrm{d}z = \sum_{k=1}^{i} \bar{Q}_{11}^{(k)}[(z^{(k+1)} - z^{(k)})u^0_{,xx} + \tfrac{1}{2}(z^{(k+1)2} - z^{(k)2})\beta_{x,xx}] + \sum_{k=1}^{i} \bar{Q}_{16}^{(k)}[v^0_{,xx}(z^{(k+1)} - z^{(k)})] \tag{18b}$$

$$\frac{\partial \tau_{xy}^{(k)}}{\partial x} = \bar{Q}_{16}^{(k)}[u^0_{,xx} + z^{(k)}\beta_{x,xx}] + \bar{Q}_{66}^{(k)}[v^0_{,xx}] \tag{19a}$$

$$\int_{\text{free}}^{z} \frac{\partial \tau_{xy}^{(k)}}{\partial x}\,\mathrm{d}z = \sum_{k=1}^{i} \bar{Q}_{16}^{(k)}[(z^{(k+1)} - z^{(k)})u_{,xx}^{0} + \tfrac{1}{2}(z^{(k+1)2} - z^{(k)2})\beta_{x,xx}] + \sum_{k=1}^{i} \bar{Q}_{66}^{(k)}[v_{,xx}^{0}(z^{(k+1)} - z^{(k)})] \quad (19b)$$

Instead of taking numerical derivatives of u^0, β_x and v^0 to obtain $u^0_{,xx}$, $\beta_{x,xx}$, and $v^0_{,xx}$, their expressions can be obtained from the governing equations of the joints (which provide expressions for $u^0_{,x}$, $\beta_{x,x}$, and $v^0_{,x}$). For example, for the single-lap and bonded doubler joints, we have the following relations [22]:

$$\begin{aligned} u_{,xx}^{0i} &= k_{1i}N_{xx,x}^{i} + k_{2i}N_{xy,x}^{i} + k_{3i}M_{xx,x}^{i} \\ \beta_{x,xx}^{0i} &= k_{4i}N_{xx,x}^{i} + k_{5i}N_{xy,x}^{i} + k_{6i}M_{xx,x}^{i}, \\ v_{,xx}^{0i} &= k_{7i}N_{xx,x}^{i} + k_{8i}N_{xy,x}^{i} + k_{9i}M_{xx,x}^{i} \end{aligned} \quad (20)$$

where k_{ji} are terms containing the laminate stiffness constants and the superscripts $i = 1, 2$ denote the adherend 1 and 2, respectively (see Mortensen [22] for details). The expressions for the x derivatives of the force and moment resultants appearing in Eq. (20) are obtained from the equilibrium equations (6) and (7) together with the adhesive constitutive relations. These expressions are, in the overlap region,

$$\begin{aligned} N_{xx,x}^{1} &= \frac{G_a}{t_a}u_0^1 + \frac{G_a t_1}{2t_a}\beta_x^1 - \frac{G_a}{t_a}u_0^2 + \frac{G_a t_2}{2t_a}\beta_x^2 \\ N_{xx,x}^{2} &= -\frac{G_a}{t_a}u_0^1 - \frac{G_a t_1}{2t_a}\beta_x^1 + \frac{G_a}{t_a}u_0^2 - \frac{G_a t_2}{2t_a}\beta_x^2 \\ N_{xy,x}^{1} &= \frac{G_a}{t_a}v_0^1 - \frac{G_a}{t_a}v_0^2, \qquad N_{xy,x}^{2} = -\frac{G_a}{t_a}v_0^1 + \frac{G_a}{t_a}v_0^2 \\ M_{xx,x}^{1} &= Q_x^1 + \frac{G_a(t_1+t_a)}{2t_a}u_0^1 + \frac{G_a t_1(t_1+t_a)}{4t_a}\beta_x^1 \\ &\quad - \frac{G_a(t_1+t_a)}{2t_a}u_0^2 + \frac{G_a t_2(t_1+t_a)}{4t_a}\beta_x^2 \\ M_{xx,x}^{2} &= Q_x^2 + \frac{G_a(t_2+t_a)}{2t_a}u_0^1 + \frac{G_a t_1(t_2+t_a)}{4t_a}\beta_x^1 \\ &\quad - \frac{G_a(t_2+t_a)}{2t_a}u_0^2 + \frac{G_a t_2(t_2+t_a)}{4t_a}\beta_x^2 \\ Q_{x,x}^{1} &= \frac{E_a}{t_a}w^1 - \frac{E_a}{t_a}w^2, \qquad Q_{x,x}^{2} = -\frac{E_a}{t_a}w^1 + \frac{E_a}{t_a}w^2 \end{aligned} \quad (21)$$

In the nonoverlap region,

$$\begin{aligned} N_{xx,x}^{i} &= 0 \\ N_{xy,x}^{i} &= 0 \qquad (i = 1, 2) \\ Q_{x,x}^{i} &= 0 \\ M_{xx,x}^{i} &= Q_x^i \end{aligned} \quad (22)$$

Thus, given the solution to the full set of governing differential equations (described in Secs. II.B–II.D), the adherend-level force and moment resultant derivatives represented by Eqs. (21) and (22) can be obtained. Then, these are substituted into Eqs. (18) and (19), allowing the integrals in Eq. (15) to be evaluated as indicated in Eqs. (18b) and (19b). Note that $\sigma_{zz}(x, z)$ is still determined via numerical integration of the results for $\tau_{xz}(x, z)$ [see Eq. (15)]. The out-of-plane stress field that results from this procedure does not suffer from the oscillations that occur when the integrals in Eq. (15) are simply evaluated numerically.

It should be noted that Eqs. (21) and (22) can have different forms for other joint types. Also note that the out-of-plane stresses solved by the above approach are based on the equilibrium equations and the in-plane stresses obtained from CLT. As such, they do not satisfy the free edge boundary conditions, where the shear stresses should equal zero.

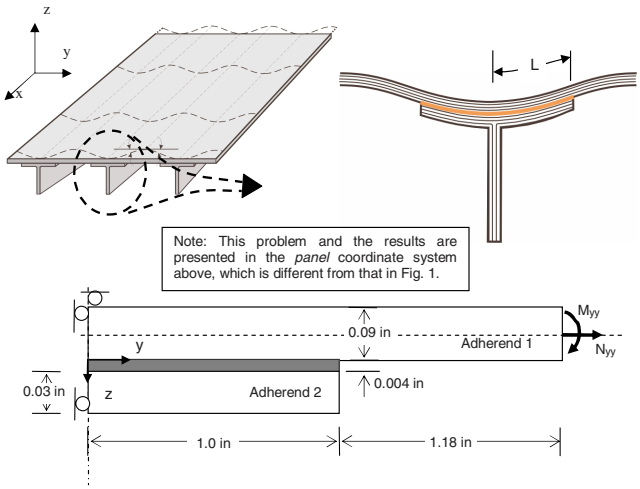

Fig. 3 Configuration of a bonded doubler joint for analysis (not to scale).

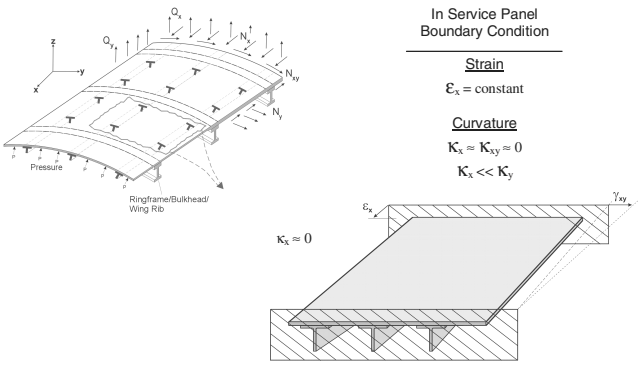

Fig. 4 Boundary conditions on an "in-service panel."

III. Numerical Examples

A. Bonded Doubler Joints with Laminated Adherends

1. *Joint Configuration*

The example results presented apply to a bonded doubler joint, which is intended to represent a section of a stiffened panel, as shown in Fig. 3. The joint uses laminated adherends with off axis plies subjected to tensile loading and bending moment loading. The configuration of the bonded doubler joint is schematically shown in Fig. 3. Adherend 1 consists of 18 plies of boron/epoxy prepreg tape and has a $[45°/-45°/0°/90°/0°/90°/45°/-45°/0°]_s$ layup with a ply thickness of 0.005 in. Adherend 2 consists of six plies of boron/epoxy prepreg tape, with a $[0°/90°/45°/-45°/90°/0°]$ layup, and a ply thickness of 0.005 in. The adherends are bonded with an epoxy adhesive film with a thickness of 0.004 in. The mechanical properties of the joint materials are given in Table 1.

2. *Boundary Conditions*

To model this problem (which is intended to simulate the in-service conditions for an airframe panel, Fig. 3) correctly, special attention must be paid to the boundary conditions. In the real situation, the bonded doubler is a part of a stiffened panel such that it is constrained in the longitudinal stiffener (x) direction. This boundary condition is imposed by either constraining the rotation and translation in the axial direction (cylindrical bending), or allowing only constant straining along this direction (generalized cylindrical bending), Fig. 4. The curvature along the longitudinal direction is small compared with that in the transverse direction. Thus, at the left side of the joint shown in Fig. 3, a symmetry boundary condition is applied, while either unit moment or tension is applied at the right side. Table 2 summarizes the boundary and loading conditions applied for each case investigated.

Table 1 Material properties used in analyses

	E_1 (Msi)	E_2 (Msi)	E_3 (Msi)	G_{12} (Msi)	G_{31} (Msi)	G_{23} (Msi)	υ_{12}	υ_{13}	υ_{23}
Boron/epoxy	32.4	3.5	3.5	1.23	1.23	1.23	0.23	0.23	0.32
Epoxy	0.445	0.445	0.445	0.165	0.165	0.165	0.348	0.348	0.348
Aluminum	10.0	10.0	10.0	3.84	3.84	3.84	0.30	0.30	0.30

Table 2 Geometry, materials, and boundary conditions of stiffened plate[a]

Layups	Loading and boundary conditions:
Adherend 1: Boron/epoxy $[45°/-45°/0°/90°/0°/90°/45°/-45°/0°]_s$	**Left face** (symmetry): $u_0 = w = \beta_y = v_0 = 0$
Adherend 2: Boron/epoxy $[0°/90°/45°/-45°/90°/0°]$	**Right face**:
Adhesive: epoxy	Case 1: $N_x = 5.71$ lb/in (1 N/mm), $Q_y = N_{yx} = M_{yy} = 0$;
	Case 2: $M_x = 0.2248$ lb in/in (1 N mm/mm), $Q_y = N_{yx} = N_y = 0$;

[a]u_0, v_0, w are the displacements of middle plane; β_y is the slope of middle plane with respect to y axis.

3. Consistency Assumptions for Finite Element Analysis Comparisons

The HyperSizer joint analysis results are compared with results from StressCheck[††], p-based finite element analysis software, to determine the through-thickness distribution of stresses. Note that this required explicit modeling of each ply in the StressCheck finite element analysis (FEA). The classical lamination theory employed by the HyperSizer method does not account for the effects of transverse shear flexibility. Therefore, to eliminate possible discrepancies this effect could cause between HyperSizer and StressCheck results, the material properties used in the FEA were modified to remove these effects. This means that in the FEA the transverse shear moduli (G_{12} and G_{13}) were set to an arbitrarily high number (1.0×10^8) and the Poisson ratios that link in-plane to out-of-plane strains (υ_{13} and υ_{23}) were set to zero. All other quantities in the FEA model were set equal to those specified in the problem defined above.

IV. Results and Discussion

A. Rapid Calculation of Interlaminar and In-Plane Stresses

One of most important features of the developed joint analysis method is the capability to calculate local interlaminar and in-plane stresses rapidly. The first example considers the joint subjected to an axial tensile load $N_y = 5.71$ lb/in. Figure 5 shows the out-of plane shear and peel stresses plotted through the thickness of the joint at several locations progressing toward the free edge of the doubler. The curves start at $y/L = 0.89$ which is about 20 ply thicknesses away from the free edge and the final curve is at $y/L = 0.998$ which is about 1/2 ply thickness away from the free edge. Notice, especially in the peel stress, that not only do the stress magnitudes vary greatly, but the character of the stress field completely changes close to the free edge. Similar plots are given for the through-the-thickness distribution of the adherend in-plane stresses at the middle point of overlap ($y/L = 0.5$) and at the free edge ($y/L = 1.0$), as shown in Fig. 6. The results show clearly the stepwise distribution of in-plane stresses due to discontinuities of material properties between plies.

B. Comparison of HyperSizer Results with Finite Element Analysis

Two cases are studied for the bonded doubler shown in Fig. 3 and the HyperSizer results are verified with FEA (StressCheck[‡‡]). In the first case, the joint is subjected to a tensile force $N_y = 5.71$ lb/in; in the second case, the joint is subjected to a bending moment $M_{yy} = 0.2246$ lb in/in. The StressCheck finite element mesh, consisting of 317 hexahedral 3-D solid elements, is shown in Fig. 7. As indicated, the mesh employed one element in the width (x) direction and one element per ply in the thickness (z) direction. Along the joint (y direction), the mesh is refined in the vicinity of the reentrant corner and at the middle of the joint. Boundary conditions imposed on the x faces, involved completely restraining the x direction displacement. The negative y face was constrained against y-direction displacement, while the tensile and moment loading was imposed on the positive y-face as a force and distributed couple, respectively. The z faces were left free aside from the middlemost element on the bottom (negative) z face, which was constrained against z-direction displacement. This final condition ensures the overall symmetry of the joint model. A fixed p level of 8 was employed in the StressCheck analyses.

Figures 8–12 show the results for case 1. Figure 8 indicates very good agreement between StressCheck and HyperSizer results for the middle-plane deflection of adherends. The ratio of span to thickness of the adherends is greater than 20:1, so that CLT should not generate large errors even if the transverse shear is considered in FEA. Figure 9 shows the comparison of StressCheck and HyperSizer results for the adhesive shear and peel stresses along the bondline. The FEA results for comparison are those at the middle of the adhesive layer. Starting at $x/L = 0$, both shear and peel stresses remain almost zero until they reach the region within 20% bondline length away from the free edge, where the peel stress first drops ("trough region") and then increases dramatically. Shear stresses

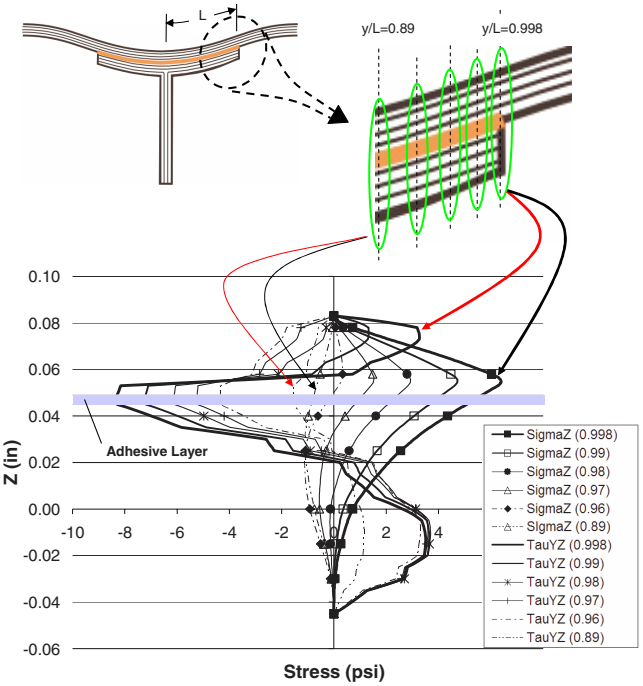

Fig. 5 HyperSizer predictions of the interlaminar stress distributions through the thickness of the joint. Parenthetical values are the y/L location of the plotted stress distribution.

[††]ESRD, Inc., 2003, Personal Communication; http://www.esrd.com, St. Louis, MO [cited 14 May 2003].

[‡‡]ESRD, Inc., http://www.esrd.com, St. Louis, MO [cited 14 May 2003].

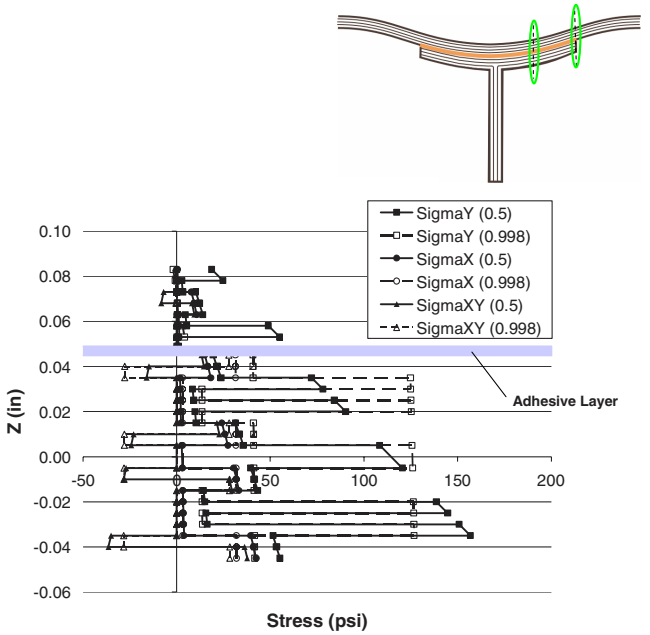

Fig. 6 HyperSizer predictions of the in-plane stress distributions through the thickness of the joint. Parenthetical values are the y/L location of the plotted stress distribution.

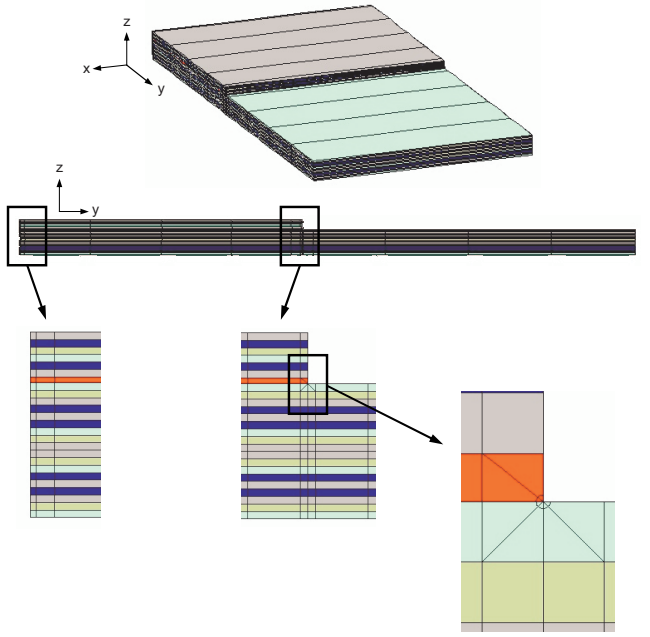

Fig. 7 StressCheck finite element mesh for the bonded composite doubler joint.

increase continuously, reaching a maximum at the free edge. The adhesive stresses predicted by HyperSizer are in good agreement with the predictions of the FEA. The shear stresses predicted by the two methods match extremely well, except for the values at the free edge, where the FEA results drops to zero but the HyperSizer solution does not. This free edge behavior is inherent to the spring-type model used for the adhesive layer in the HyperSizer joint analysis. The peel stresses predicted by the two methods match generally well, but it appears that the HyperSizer's solution in the "trough" region is more conservative than FEA's. The maximum pointwise difference between the two methods for the peel stress in the trough region is as high as 50%. Since the transverse shear effect of adherends has been artificially ruled out in FEA, this error is likely caused by the spring-model used in the HyperSizer joint analysis for the adhesive layer.

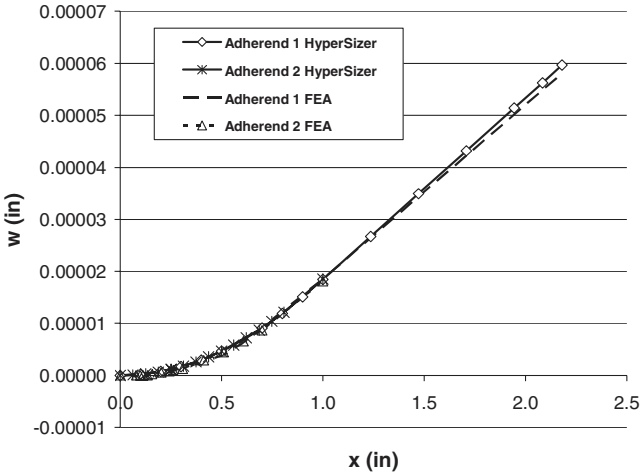

Fig. 8 Middle-plane deflection of adherends of the bonded doubler subjected to tension ($N_{yy} = 5.7$ lb/in.).

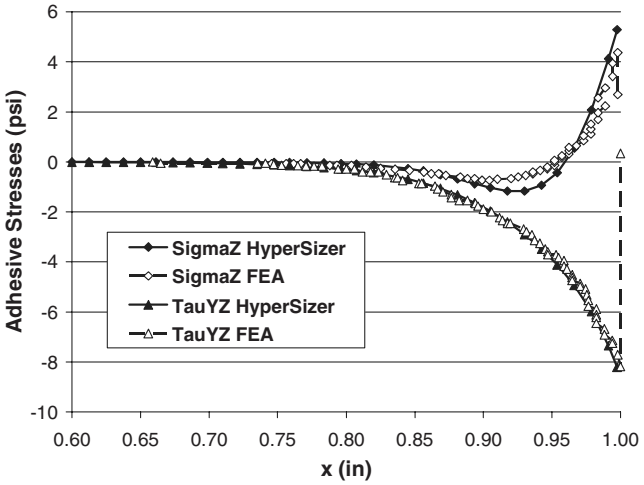

Fig. 9 Adhesive shear and peel stresses in the bonded doubler subjected to tension ($N_{yy} = 5.7$ lb/in.).

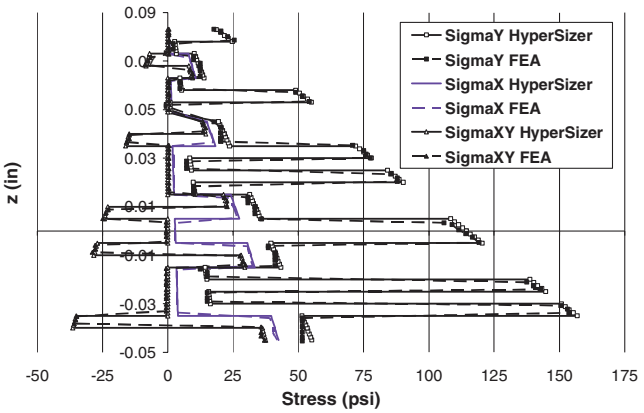

Fig. 10 Through-the-thickness distribution of in-plane stresses at $y/L = 0.5$ in the bonded doubler subjected to tension ($N_{yy} = 5.7$ lb/in.).

Figure 10 shows the comparison of the StressCheck and HyperSizer predictions for the through-the-thickness distribution of in-plane stresses in the adherends. It can be seen that the HyperSizer results match well with the FEA results. Figure 11 shows the comparison of StressCheck and HyperSizer predictions for the through-the-thickness distribution of out-of-plane stresses in the adherends near the free edge, i.e., $y/L = 0.89$. Good agreement is

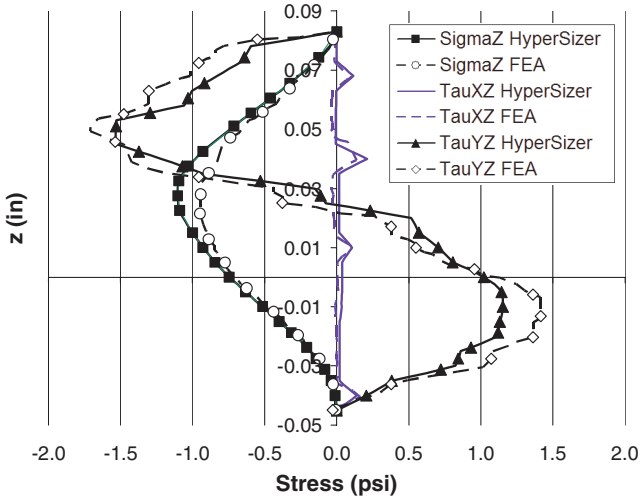

Fig. 11 Through-the-thickness distribution of out-of-plane stresses at $y/L = 0.89$ in the bonded doubler subjected to tension ($N_{yy} = 5.7$ lb/in.).

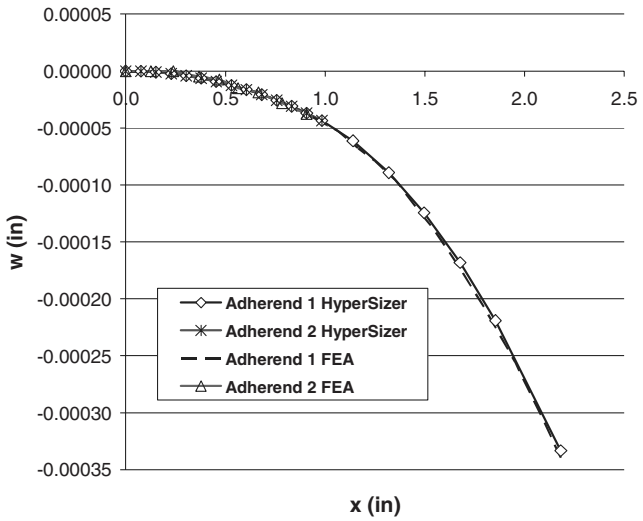

Fig. 12 Middle-plane deflection of adherends of the bonded doubler subjected to bending moment ($M_{yy} = 0.2248$ in.-lb/in.).

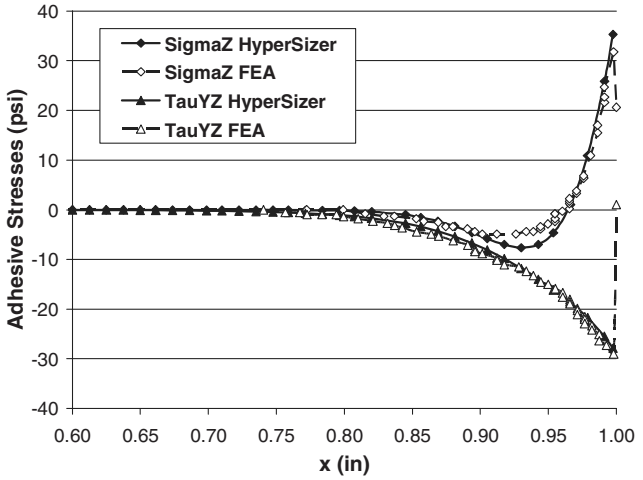

Fig. 13 Adhesive shear and peel stresses in the bonded doubler subjected to bending moment ($M_{yy} = 0.2248$ in.-lb/in.).

achieved between HyperSizer and FEA, and the transverse shear stress shows surprisingly good agreement in particular. At $y/L = 0.89$, the HyperSizer solution for the peel stress does not vary much from that of FEA. Also, as can be seen from the

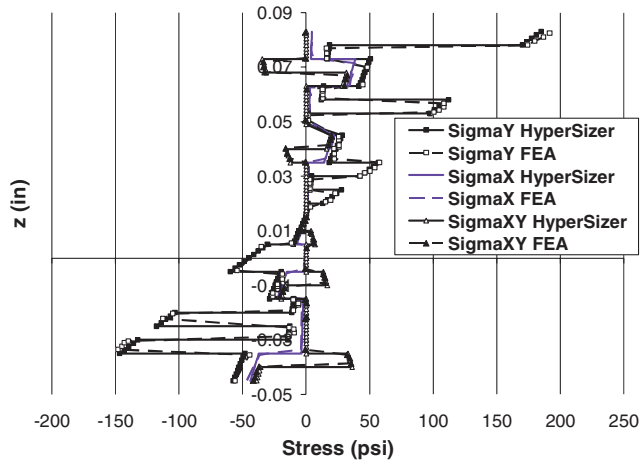

Fig. 14 Through-the-thickness distribution of in-plane stresses at $y/L = 0.50$ in the bonded doubler subjected to bending moment ($M_{yy} = 0.2248$ in.-lb/in.).

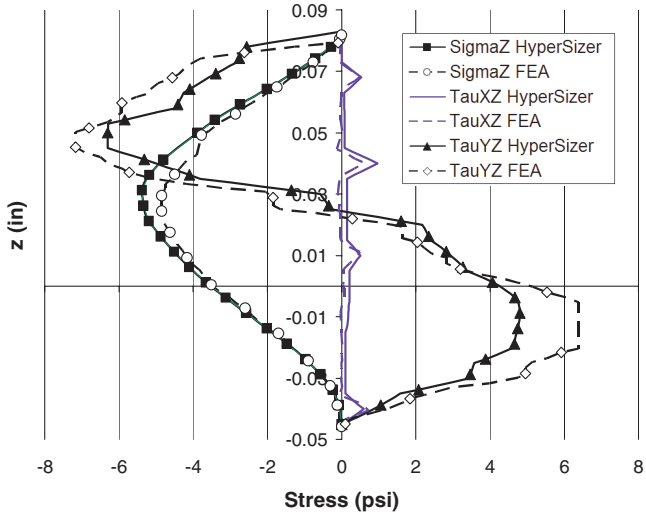

Fig. 15 Through-the-thickness distribution of out-of-plane stresses at $y/L = 0.89$ in the bonded doubler subjected to bending moment ($M_{yy} = 0.2248$ in.-lb/in.).

equilibrium equations (15), the longitudinal shear stress τ_{xz} is obtained from the through-the-thickness integration of derivative of σ_{xx}, while peel stress σ_{zz} is a result from the integration of derivative of τ_{xz}. As such, the error in τ_{xz} may be accumulated and brought into the resulting peel stress σ_{zz} integration, which generally results in larger error. Recall that the finite element model was artificially stiffened by reducing the transverse shear deformation of adherends and the Poisson effect as to match as much as possible with HyperSizer's assumption based on CLT. Thus, it is likely that most of the differences observed in the analysis between HyperSizer and FEA result from the spring model for the adhesive layer.

Figures 12–15 show the comparison of the same results of HyperSizer and StressCheck for the joint under an applied bending moment $M_{yy} = 0.2248$ lb in/in. Again, it shows that excellent agreement was obtained for the in-plane stresses, while good agreement was reached for the out-of-plane stresses as well as the adhesive stresses. In both cases, it appears that the spring model used for the adhesive layer affects the results of out-of-plane stresses more than those of in-plane stresses. Recently, Mortensen and Thomsen [24] have shown that replacing the spring model with a high-order theory enables better agreement for the adhesive stresses with FEA solutions, especially in the vicinity of free edges. Thus, it is expected the adhesive stresses and adherend interlaminar stresses would be improved through introduction of a more realistic model for the adhesive.

Table 3 Comparison of HyperSizer method to Hart-Smith method for bonded joint analysis

	Bonded joint analysis by Hart-Smith [14–19]	Bonded joint analysis by HyperSizer
Solver	1-D closed-form solution using beam theory	A closed-form solution based on Mortensen's [22] unified approach and modification
Joint types	Conventional joints: Single-lap, double-lap, scarfed, and stepped joints	Conventional joints: Single-lap, double-lap, scarfed, and stepped joints [adherend can be straight or scarfed (ply-dropoff)]
Loads and effects	N_x, Q_x, M_{xx}	N_x, Q_x, M_{xx}, N_{xy} (N_y, Q_y, M_{yy} and M_{xy} are reaction forces). Also can enter strains and curvatures and in any combination with the forces and moments
	1. Temperature change 2. Adherend imbalance 3. Defects in *bond layer*, such as porosity, thickness variation are considered, etc.	1. Temperature change 2. Moisture in laminates
Adherends	Linear elastic homogenized beams, no transverse deformation is accommodated	Linear elastic classical laminates (could be asymmetric and unbalanced), no transverse deformation is yet accommodated but will be in a future release
	Output: 1. Longitudinal normal stress and strain, as well as displacement (u_0, w) 2. Interlaminar stresses are not available	Output: 1. In-plane stresses, strains, and displacement (u_0, v_0, w) 2. Out-of-plane (interlaminar) stresses are calculated.
Adhesive	1. Shear spring only 2. Elastic-perfectly plastic material	1. 2-D isotropic linear elastic spring 2. Several nonlinear material representations 3. High-order theory (to be developed) 4. Spew fillet effect (to be developed)
	Output: Shear (longitudinal only) stress for most joint types. A simplified method is proposed for solving for the peel stress, which is decoupled from the adhesive shear stress	Output: Shear (longitudinal and transverse) and peel stresses, which are constants through the thickness by using the spring model, but may vary if using high-order theory
Convergence of solution	Have stability/convergence problems with stepped-lap joints	Convergence is more robust

V. Comparison to Other Analytical Methods

The HyperSizer joint analysis method offers many advantages over traditional analytical methods for bonded joint analysis in that it is capable of handling more general situations, including various joint configurations, both linear and nonlinear adhesive, asymmetric and unbalanced laminates and more general loading and boundary conditions, and most importantly, it is capable of computing local in-plane and interlaminar stresses in composite adherends. The traditional analytical methods have undergone continuous development over decades. Among all the methods, there are two analytical methods which have been well-known to aerospace industry: Hart-Smith method [14–19] and Erdogan method [20,26]. We briefly described the two methods in Sec. I. In the following, these two methods are compared with the HyperSizer joint analysis method in a more detailed manner in order to highlight its advantages.

A. Comparison to Hart-Smith Method

The Hart-Smith method has been developed based on Goland and Reissner's [13] theory for a single-lap joint in which the two adherends were considered as beams and the adhesive layer in the joint was treated as a special kind of "connecting spring" acting between the two beams. Hart-Smith not only extended this approach to a variety of joint types, such as double-lap, scarf and stepped-lap joints, but also modified the approach to incorporate many types of effects such as adhesive plasticity, thermal mismatch and stiffness imbalance. Hart-Smith's efforts resulted in efficient computer codes (one is known as A4EI) for performing parametric studies on a wide array of joint configurations. In addition to the stress analysis, Hart-Smith also characterized failure modes of bonded joints and developed a series of engineering design rules.

Compared with the Hart-Smith method, the new HyperSizer method has the following major advantages. First, the new method models the adherends as general classical laminates, which can accommodate multiaxial loads and more general boundary conditions, such as N_x (or u_0), Q_x (or w), M_{xx} (or β_x), and N_{xy} (or v_0), as well as the generation of the reaction forces and moments M_{yy}, M_{xy}, N_y, and Q_y. In contrast, Hart-Smith method models the adherends as 1-D beams, which can only accommodate N_x (or u_0), Q_x (or w), and M_{xx}. Second, the HyperSizer method can determine the adhesive stresses in terms of the longitudinal shear stress, transverse shear stress and transverse normal (peel) stress. However, Hart-Smith's solution focused on the longitudinal shear stress, giving either the elastic or elastic-perfectly plastic solutions, while neglecting the adhesive peel stress. Hart-Smith believed that the adhesive peel stress could be reduced by appropriate design of the joint and thus should not be an issue. Even though Hart-Smith did not include the peel stress calculation in the joint analysis computer program A4EI, he gave a simplified method for calculating adhesive peel stress in his NASA report for double-lap joints [14]. This simplified method assumes that the adhesive shear stress is constant in the presence of peel stress, so that the peel stress solution is totally uncoupled from the shear stress. This assumption is unrealistic and could lead to large errors in the solution for the adhesive peel stress. Third, the shear/tension spring model employed for the adhesive layer is more capable than Hart-Smith's adhesive model in that it can be extended to high-order theory and inclusion of spew fillet effect [22]. Fourth, the Hart-Smith method has convergence and precision problem, especially for stepped-lap joints. The convergence difficulties are problem dependent, being more severe for brittle (high modulus) adhesives. The underlying difficulty is one of numerical accuracy loss in the presence of extremely high adhesive shear stress gradients at both ends of each of the outer steps. In contrast, HyperSizer's joint solutions have very good convergence and accuracy due to the multisegment integration method [22] used to solve the differential equations. This numerical method generates very stable solutions for stepped or scarfed joints with either linear or nonlinear adhesives (not just restricted to elastic-perfectly plastic materials). Finally, the HyperSizer method can solve for both in-

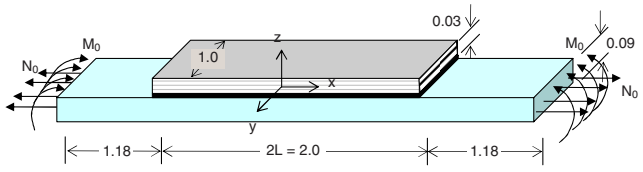

Fig. 16 Stiffened plate (bonded doubler) geometry analyzed by Delale et al. [20]. All dimensions are in.

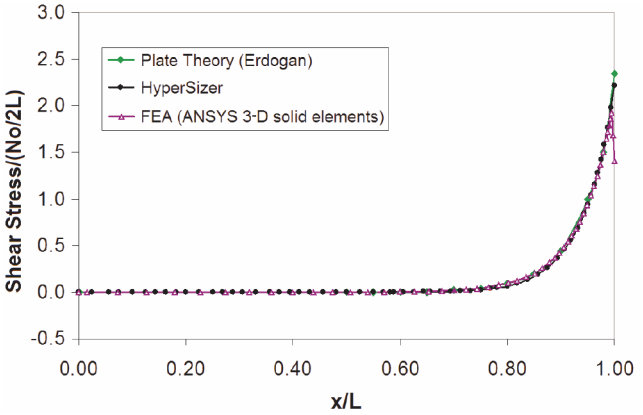

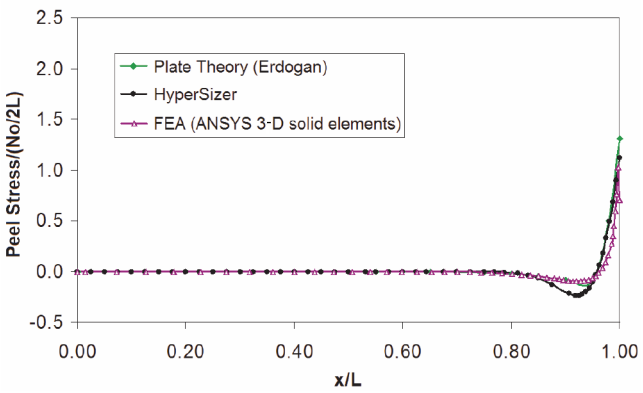

Fig. 17 Normalized adhesive stresses in the bonded doubler subjected to tension.

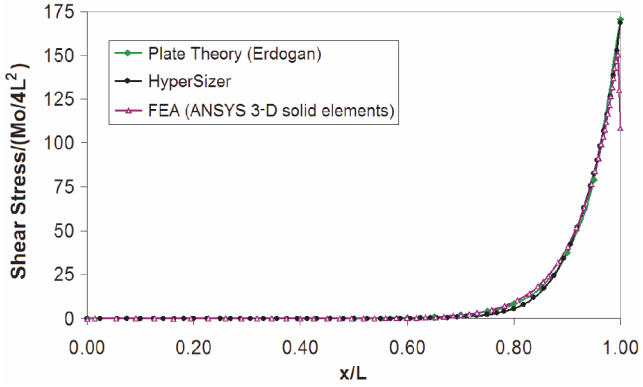

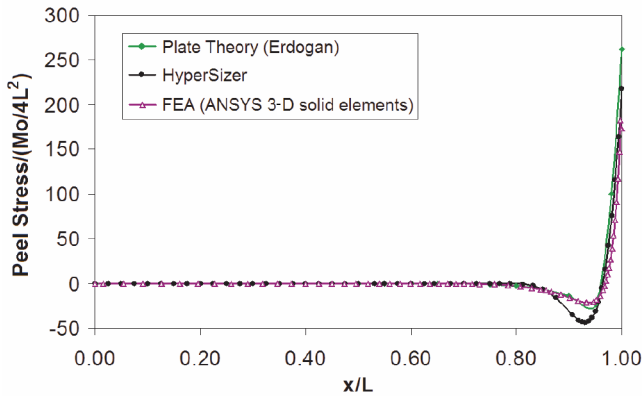

Fig. 18 Normalized adhesive stresses in the bonded doubler subjected to bending moment.

plane and out-of-plane stresses in the adherends, while the Hart-Smith method cannot. This multiaxial stress analysis capability enables failure analysis for composite adherends which commonly suffer interlaminar failures. Comparison of the HyperSizer joint analysis method to the Hart-Smith method is summarized in Table 3.

B. Comparison to Erdogan's Method and FEA

The work of Erdogan (and coworkers [20,26]) on bonded joint analysis resulted in a unified analytical approach for several joint configurations: stepped-lap joints, single-lap joints, and bonded doublers. The most prominent feature of the Erdogan method is the application of plate theory to joint analysis. However, compared with the HyperSizer method, the Erdogan method has the following shortcomings: 1) the adherends are orthotropic plates and thus can only accommodate the loads of N_x (or u_0), Q_x (or w), and M_{xx}; 2) the Erdogan method does not solve for the out-of-plane stresses of adherends so that it can not be used to predict adherend interlaminar failures. To further explore the differences between the two methods, in the following an example problem for a bonded doubler studied by Delale et al. [20] is selected to compare the Erdogan method and the HyperSizer joint analysis method to FEA.

The problem definition and coordinate system for the joint geometry is shown in Fig. 16. The plate material is aluminum, while the flange material is a unidirectional orthotropic Boron/Epoxy composite. The two adherends are bonded using epoxy adhesive, with a thickness of 0.004 in. The material properties are listed in Table 1. Symmetric boundary conditions are applied at the middle cross section (i.e., $x = 0$) such that only one-half of the geometry shown in Fig. 16 is analyzed, and a tension or moment load is applied at the plate's right edge.

Figures 17 and 18 show the normalized adhesive longitudinal shear and peel stresses for the joint under tension and moment, respectively. The shear and peel stresses from the HyperSizer and Erdogan methods generally match very well with finite element results, except for the peak values near the free edge. The Erdogan solution exhibits a larger difference for the peak stress at the free edge compared with the FEA result, while HyperSizer has the larger difference for the peel stress in the "trough region." HyperSizer's difference in trough region has been observed in the example in Sec. III, in which case the transverse shear effect of the adherends was artificially reduced in the finite element models. As a result, we have attributed those discrepancies to the spring model used for the adhesive layer. In the present case, the transverse effect in the adherends is not pronounced due to the large span-to-thickness ratio of the adherends. Thus the adhesive model may play an important role in causing the discrepancy in the HyperSizer peel stress in the trough region. It should be noted that the Erdogan method employed an "improved spring model" for the adhesive, which accounts for the effect of longitudinal strain of the adhesive in addition to the shear and peel strain. Therefore, improvement of the peel stress in the trough region may be attributable to the usage of this improved adhesive model. As such, HyperSizer's results could also be improved if the spring model could be modified or replaced, for instance, by the high-order theory as suggested in the previous section.

VI. Conclusion

A method for multiaxial stress analysis of composite bonded joints has been developed. Compared to other analytical methods used for bonded joint analysis, the present method is capable of handling more general situations, including various joint geometries, both linear and nonlinear adhesive, asymmetric and unbalanced laminates, and more general loading and boundary conditions. The new method is developed based on Mortensen's unified approach, but it has been considerably extended and modified to enable accommodation of transverse in-plane straining and hygrothermal loads and, most importantly, to be able to compute local in-plane and interlaminar stresses throughout the adherends. It has been implemented within the commercially available HyperSizer® stiffened structural analysis software package. The present investigation employs HyperSizer's new joint analysis capability to model an adhesively bonded composite bonded doubler joint,

which represents a section of an aerovehicle stiffened panel. Results have been compared with *p*-based finite element results (StressCheck), *h*-based finite element results (ANSYS), and the analytical solution of Erdogan and coworkers [20–26]. Good agreement has been obtained between the HyperSizer method and these other joint analysis methods. The method thus appears to be efficient and generally accurate for analysis of composite bonded joints. It represents a very capable tool for preliminary design, where fast estimates of stress fields, as well as joint strengths and margin of safety are needed.

Acknowledgement

This work was partially supported by Air Force Research Laboratory (AFRL) under Contract F33615-02-C-3216.

References

[1] Collier Research Corp., HyperSizer Structural Sizing Software, Hampton, VA, 2003.

[2] Kairouz, K. C., and Matthews, F. L., "Strength and Failure Modes of Bonded Single Lap Joints Between Cross-Ply Adherends," *Composites*, Vol. 24, No. 6, 1993, pp. 475–484.

[3] Shenoi, R. A., and Hawkins, G. L., "An Investigation into the Performance Characteristics of Top-Hat Stiffener to Shell Plating Joints," *Composite Structures*, Vol. 30, No. 1, 1995, pp. 109–121.

[4] Tsai, M. Y., Morton, J., and Matthews, F. L., "Experimental and Numerical Studies of a Laminated Composite Single-Lap Adhesive Joint," *Journal of Composite Materials*, Vol. 29, No. 9, 1995, pp. 1254–1275.

[5] Yamazaki, K., and Tsubosaka, N., "A Stress Analysis Technique for Plate and Shell Built-Up Structures with Junctions and Its Application to Minimum-Weight Design of Stiffened Structures," *Structural Optimization*, Vol. 14, No. 2–3, 1997, pp. 173–183.

[6] Tong, L., "An Assessment of Failure Criteria to Predict the Strength of Adhesively Bonded Composite Double Lap Joints," *Journal of Reinforced Plastics and Composites*, Vol. 16, No. 8, 1997, pp. 699–713.

[7] Li, G., Lee-Sullivan, P., and Thring, R. W., "Nonlinear Finite Element Analysis of Stress and Strain Distributions Across the Adhesive Thickness in Composite Single-Lap Joints," *Composite Structures*, Vol. 46, No. 4, 1999, pp. 395–403.

[8] Apalak, Z. G., Apalak, M. K, and Davies, R., "Analysis and Design of Tee Joints with Double Support," *International Journal of Adhesion and Adhesives*, Vol. 16, No. 3, 1996, pp. 187–214.

[9] Krueger, R., Cvitkovich, M. K., O'Brien, T. K., and Minguet, P. J., "Testing and Analysis of Composite Skin/Stringer Debonding Under Multi-Axial Loading," NASA Langley Research Center, NASA/TM-1999-209097, February 1999.

[10] Krueger, R., Minguet, P. J., and O'Brien, T. K., "A Method for Calculating Strain Energy Release Rates in Preliminary Design of Composite Skin/Stringer Debonding Under Multi-Axial Loading," NASA Langley Research Center, NASA/TM-1999-209365, July 1999.

[11] Bogdanovich, A. E., and Kizhakkethara, I., "Three-Dimensional Finite Element Analysis of Double-Lap Composite Adhesive Bonded Joint Using Submodeling Approach," *Composites, Part B*, Vol. 30, No. 6, 1999, pp. 537–551.

[12] Volkersen, O., "Die Nietkraftoerteilung in Ubeansprunchten Nietverbindungen mit Konstanten Loshonquerschnitten" *Luftfahrt-forschung*, Vol. 15, No. 1/2, 1938, pp. 41–47.

[13] Goland, M., and Reissner, E., "The Stresses in Cemented Joints," *Journal of Applied Mechanics*, Vol. 11, No. 1, 1944, pp. A17–A27.

[14] Hart-Smith, L. J., "Adhesive-Bonded Double-Lap Joints," NASA Langley Research Center, NASA-CR-112235, January 1973.

[15] Hart-Smith, L. J., "Adhesive-Bonded Single-Lap Joints," NASA Langley Research Center, NASA-CR-112236, January 1973.

[16] Hart-Smith, L. J., "Adhesive-Bonded Scarf and Stepped-Lap Joints," NASA Langley Research Center, NASA-CR-112237, January 1973.

[17] Hart-Smith, L. J., "Adhesive Bond Stresses and Strains at Discontinuities and Cracks in Bonded Structures," *Journal of Engineering Materials and Technology*, Vol. 100, No. 1, 1978, pp. 16–24.

[18] Hart-Smith, L. J., "Differences Between Adhesive Behavior in Test Coupons and Structural Joints," Douglas Aircraft Company Paper 7066, Long Beach, CA, March 1981.

[19] Hart-Smith, L. J., "Design Methodology for Bonded-Bolted Composite Joints," Douglas Aircraft Company, United States Air Force Contract Rept. AFWAL-TR-81-3154, Vols. 1, 2, Wright-Patterson Air Force Base, OH, February 1982.

[20] Delale, F., Erdogan, F., and Aydinoglu, M. N., "Stresses in Adhesively Bonded Joints: A Closed-Form Solution," *Journal of Composite Materials*, Vol. 15, May 1981, pp. 249–271.

[21] Oplinger, D. W., "A Layered Beam Theory for Single-Lap Joints," Army Materials Technology Laboratory, Rept. MTL TR 91-23, 1991.

[22] Mortensen, F., "Development of Tools for Engineering Analysis and Design of High-Performance FRP-Composite Structural Elements," Ph.D. Dissertation, Institute of Mechanical Engineering, Aalborg University (Denmark), Special Report No. 37, 1998.

[23] Mortensen, F., and Thomsen, O. T., "Analysis of Adhesive Bonded Joints: A Unified Approach," *Composites Science and Technology*, Vol. 62, No. 7–8, 2002, pp. 1011–1031.

[24] Mortensen, F., and Thomsen, O. T., "Coupling Effects in Adhesive Bonded Joints," *Composite Structures*, Vol. 56, No. 2, 2002, pp. 165–174.

[25] Collier Research Corp., "Consistent Structural Integrity and Efficient Certification with Analysis," Air Force Small Business Innovative Research, Rept. F33615-02-C-3216, Vol. 1–3, 2004.

[26] Erdogan, F., and Ratwani, M., "Stress Distribution in Bonded Joints," *Journal of Composite Materials*, Vol. 5, July 1971, pp. 378–393.

B. Sankar
Associate Editor